Journal of Applied Polymer Science

Preparation and characterization of hydrophilic and antifouling poly(ether sulfone) ultrafiltration membranes modified with Zn–Al layered double hydroxides

Yu Zhao,[1,2] Nana Li,[1] Fangzhu Yuan,[1] Haiding Zhang,[1] Shengji Xia[1,2]

[1]State Key Laboratory of Pollution Control and Resources Reuse, Tongji University, Shanghai 200092, China

[2]Key Laboratory of Yangtze River Water Environment (Ministry of Education), Tongji University, Shanghai 200092, China

Correspondence to: S. Xia (E-mail: xiashengji@tongji.edu.cn)

ABSTRACT: Zn–Al layered double hydroxide (LDH)-entrapped poly(ether sulfone) (PES) ultrafiltration membranes with four different weight percentages, 0.5, 1.0, 2.0, and 3.0%, were prepared by a phase-inversion method. Characterization by scanning electron microscopy, atomic force microscopy and contact angle (CA), equilibrium water content, porosity, average pore size, mechanical strength, and ζ potential measurement were used to evaluate the morphological structure and physical and chemical properties of membranes. Static protein adsorption, filtration, and rejection experiments were conducted to study the antifouling properties, water permeability, and removal ability of the modified membranes. The results show that significant change occurred in the membrane morphology and that better hydrophilicity, water permeability, and antifouling ability were also achieved for the PES/LDH membranes when a proper amount of LDH was used. For example, the CA value decreased from 66.60 to 50.21°, and the pure water flux increased from 80.21 to 119.10 L m^{-2} h^{-1} bar^{-1} when the LDH loading was increased from 0 to 2.0 wt %. © 2016 Wiley Periodicals, Inc. J. Appl. Polym. Sci. **2016**, *133*, 43988.

KEYWORDS: membranes; nanoparticles; nanowires and nanocrystals; properties and characterization; separation techniques; synthesis and processing

Received 7 March 2016; accepted 29 May 2016

DOI: 10.1002/app.43988

INTRODUCTION

The application of membrane technology has been an attractive option for water treatment over the last 3 decades because it has advantages that include a reduction in the number of unit operations, selective separation, high removal efficiency, continuous and antomatic operation, and low operation cost.[1–4] Therein, the use of ultrafiltration membranes, in which the membrane material properties are vital, is one of the most popular techniques.[5] Poly(ether sulfone) (PES) has gained tremendous attention as a promising polymeric membrane material because of its outstanding chemical and physical properties (e.g., thermal stability, pressure, and heat resistance).[6,7] However, the inherent hydrophobicity of PES and the pressure-driven properties of ultrafiltration cause the poor antifouling properties of the ultrafiltration process with PES membranes. Membrane-fouling results from the deposition, adsorption, or adhesion of foulants such as protein molecules onto membranes, and the entrapment or aggregation of foulants in the pores can increase the hydraulic resistance to water flow and, thus, decrease the water permeability and economic efficiency. This restricts the practical application of the membranes in water treatment.[8–10]

Although membrane cleaning methods, including physical, chemical, and biological cleaning methods, can effectively remove contaminants on the surface or in the membranes, they complicate the operation process, affect the membrane service life, and increase the operating costs of membrane treatment.[11] Therefore, various methods to improve the antifouling properties of PES membranes have been studied by researchers. For example, studies on interfacial polymerization,[12,13] surface graft polymerization,[14] ultraviolet irradiation,[15] coating,[16] and blending[5,17,18] have been carried out with different membrane modifiers. The blending of inorganic materials into membranes as modifiers has been one focus area of this research.

Layered double hydroxide (LDH) is a typical anionic nanoclay derived from the partial isomorphous substitution of trivalent cations for divalent ones, and it has a brucitelike structure.[19] LDH has attracted much attention because of its wide and useful applications in adsorption,[20] catalysis,[21] ion exchange,[22] and so forth. The two-dimensional nanoplates can be expressed by the following general formula:

$$\left[M^{II}{}_{1-x}M^{III}{}_{x}(OH)_2\right]^{x+}\cdot\left(A^{n-}{}_{x/n}\right)\cdot mH_2O$$

where M^{II} and M^{III} are the divalent and trivalent cations, respectively, and A^{n-} represents the interlayer anions.[23] Until now, various inorganic nanofillers, such as zeolite,[24] ZnO,[25] and SiO_2,[26] have been used in membrane modification because of the good hydrophilicity or porous structure of these nanofillers, but few studies have focused on the preparation of polymer membranes modified with LDH.[27]

The objective of this study was to prepare a neat PES membrane and Zn–Al LDH-incorporated PES membranes by a phase-inversion method and to systematically investigate the effects of the LDH content in the dope solution (0–3.0 wt %) on the PES membrane properties. Different characterizations, including scanning electron microscopy (SEM), atomic force microscopy (AFM), contact angle (CA), porosity, static protein adsorption, and rejection experiments were carried out to evaluate the morphology, hydrophilicity, water permeation, and antifouling properties of the membranes.

EXPERIMENTAL

Materials

To prepare Zn–Al LDH, $Zn(NO_3)_2{\cdot}6H_2O$, $Al(NO_3)_3{\cdot}9H_2O$, NaOH, and $NaNO_3$ were purchased from Aladdin Industrial Co. (China) and were used as received. PES (3100P; weight-average molecular weight = 35,000 Da) was obtained from Solvay Co., Ltd., and was dried at 60 °C overnight in an oven before dope preparation. Polyvinylpyrrolidone (PVP; K30; weight-average molecular weight = 40,000 Da, Sinopharm Chemical Reagent Co., Ltd., China) was purchased and was used as an additive and pore former. The solvent of the casting solution was *N,N*-dimethylacetamide (DMAc; analytical-reagent grade, Aladdin Industrial Co., China, purity = 99%). Bovine serum albumin (BSA) and lysozyme (LYS) were purchased from Aladdin Industrial Co. and were used for the static protein adsorption and rejection experiments. Deionized (DI) water (18.2 MΩ cm at 25 °C) was supplied by a water-purification system (Milli-Q, Millipore Co.) to prepare all of the solutions needed in this study.

Preparation of the Zn–Al LDH and Membranes

Zn–Al LDH was synthesized by the coprecipitation method. It was prepared by the slow addition of a solution containing $Zn(NO_3)_2{\cdot}6H_2O$ (0.2 mol/L) and $Al(NO_3)_3{\cdot}9H_2O$ (0.1 mol/L) and a solution containing NaOH (0.48 mol/L) and $NaNO_3$ (0.2 mol/L) into DI water under vigorous stirring at room temperature. The pH value of the mixture was kept at 8.0 in this process. After 1 h of stirring, the suspension was maintained at 70 °C for 12 h, washed many times with DI water, and centrifuged at 5000 rpm for 10 min until the pH was 7.0 ± 0.2. The obtained solid was dried in an oven at 105 °C for 12 h and ground to obtain Zn–Al LDH for further use.

The phase-inversion method was used to prepare flat-sheet PES membranes. Different amounts of the prepared LDH were dosed into the DMAc solvent and dispersed under constant shaking and ultrasonic treatment. Then, PES and PVP were dissolved in the suspension mentioned previously and stirred at 60 °C for 48 h to ensure homogeneous mixing. To remove air bubbles, the casting solution was kept at room temperature for 24 h. Then, it was cast onto a glass plate with a doctor blade with an air gap set at 150 μm. After 30 s of solvent evaporation, the membrane was immersed into a water bath for 10 min and transferred to a DI water bath for at least 24 h at room temperature to remove the residual solvent. A digital viscometer (NDJ-8S, Shanghai Fangrui Instrument Co., Ltd., China) was used to measure the viscosity of the pure and LDH-incorporated casting solutions. Table I lists the compositions of all of the casting solutions.

Table I. Compositions of the Casting Solutions

Membrane type	PES (g)	PVP (g)	LDH (g)	DMAc (g)
PES-0	3.3	0.3	0	11.4
PES-1	3.3	0.3	0.075	11.325
PES-2	3.3	0.3	0.15	11.25
PES-3	3.3	0.3	0.3	11.1
PES-4	3.3	0.3	0.45	10.95

Characterization

Field emission scanning electron microscopy (FESEM; Ultra 55, Carl Zeiss Co., Germany) and transmission electron microscopy (TEM; CM200, FEI, The Netherlands) were used to characterize the morphology of Zn–Al LDH. The LDH particles were sputtered with gold to increase their conductivity before they were investigated by FESEM.

SEM (Phenom Pro, Phenom World, Inc., The Netherlands) was used to examine the cross-sectional morphologies of the PES membranes. To obtain their cross-sectional morphologies, the membrane samples were dried in an oven at 40 °C for 12 h and fractured in liquid nitrogen before viewing. FESEM–energy-dispersive X-ray (EDX) mapping was used to investigate the distribution of nanoparticles. AFM (Multimode 8, Bruker Corp.) was used to observe the surface morphology and roughness of the prepared PES membranes. The static CAs between water and the membrane surface were measured with an optical CA meter (Attension Theta Lite, Biolin Scientific Co., Ltd., Sweden) to examine the hydrophilicity of the membranes.

The equilibrium water content (EWC) of the prepared PES membrane was calculated as follows[28]:

$$EWC = [(m_w - m_d)/m_w] \times 100\% \quad (1)$$

where m_w is the wet weight of the PES membrane measured after the excess water on the membrane surface is wiped and m_d is the dry weight of the membrane measured after the samples are dried in an oven.

The membrane porosity was determined with a gravimetric method and was calculated with the following equation:[29]

$$\text{Membrane porosity} = (m_w - m_d)/(A_0 L \rho_w) \quad (2)$$

where m_w and m_d are the weights of the wet and dry membranes, respectively; ρ_w is the density of water; and A_0 and L represent the surface area and thickness, respectively, of the membrane.

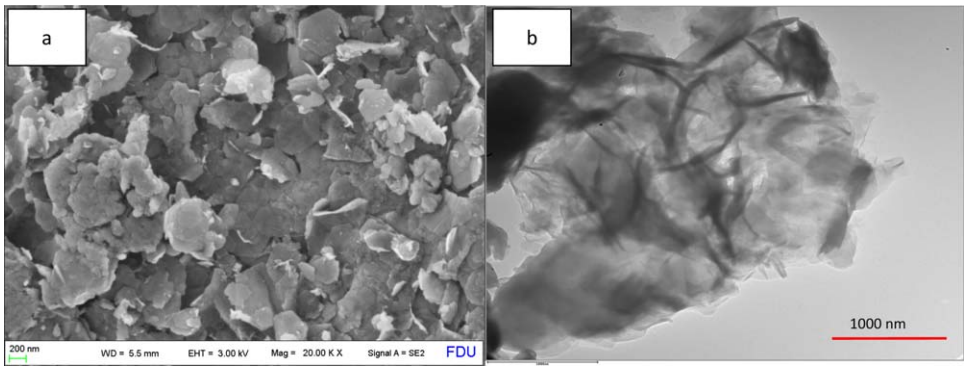

Figure 1. (a) FESEM and (b) TEM images of Zn–Al LDH. [Color figure can be viewed in the online issue, which is available at wileyonlinelibrary.com.]

The mechanical properties of membranes, including the tensile strength and elongation at break, were measured with a universal testing machine (CMT-4104, Shenzhen SANS Test Machine Co., Ltd., China) equipped with a 50-N load cell. The strain speed was 10 mm/min.

The ζ potentials of the PES membranes were also measured to investigate the charge properties of the membranes. A streaming potential instrument (SurPASS, Anton Paar, Austria) was used to examine the ζ potentials of the membranes at 25.0 ± 0.5 °C in a 1.0 m*M* KCl solution over the pH range 5–11.

On the basis of the membrane porosity and pure water flux, the value of the average pore radius (r_m) was obtained by a revised form of the Guerout–Elford–Ferry equation:[30]

$$r_m = \sqrt{\frac{(2.90-1.75\varepsilon)8\eta h Q}{\varepsilon P A}} \quad (3)$$

where ε is the porosity of the membrane, η is the viscosity of water, h is the thickness of the membrane, Q is the water flux per unit of time, P is the operational pressure, and A is the effective area of the membrane.

Membrane Performance Evaluation

A dead-end cell filtration system was used to evaluate the membrane permeation performance. PES membranes were put at the bottom of the solvent-resistant stirred cell (XFUF07601, Millipore Corp.). The effective membrane area was 34.21 cm^2, and the pressure was provided by a nitrogen gas cylinder. Before measurements, the prepared membranes were initially prepressurized for 30 min at 0.4 MPa. Then, the pure water flux was recorded under a transmembrane pressure of 0.1 MPa and was calculated with the following equation:

$$\text{Pure water flux} = Q/A\Delta t \quad (4)$$

where Q is the volume of the permeate pure water (L), A is the effective area of the membrane (m^2), and Δt is the permeation time (h).

BSA and LYS solutions in phosphate buffer (1.0 g/L, pH 7.4) were used to explore the rejection properties of the membranes. The rejection experiments were carried out under 0.1 MPa, and the protein concentrations in the feed and permeation solutions were measured with an ultraviolet–visible spectrophotometer (Lengguang-UV765, Shanghai INESA Co., Ltd., China) at 280 nm.[31]

To investigate the fouling resistance properties of the prepared PES membranes, BSA and LYS solutions with a concentration of 1.0 g/L (pH 7.4, in 10 mmol phosphate buffer) were also prepared as model proteins for the static protein adsorption experiments. In detail, a membrane sample with a size of 2.5 × 2.5 cm^2 was placed into 10 mL of BSA or LYS solution at 25 °C for 12 h at a stirring speed of 100 rpm to reach adsorption equilibrium. An ultraviolet–visible spectrophotometer (Lengguang-UV765,Shanghai INESA Co. Ltd., China) was used to measure the concentrations of the protein solution before and after adsorption at a wavelength of 280 nm.

RESULTS AND DISCUSSION

Morphology of the Zn–Al LDH

FESEM and TEM provided intuitive information for the samples. Figure 1 presents the FESEM and TEM images of Zn–Al LDH. The individual LDH platelet had a thin, platelike lamellar morphology and a hexagonal structure, with an average size of 0.5 μm; this was similar to results from other researchers.[20] The well-recognized single or few layers of LDH guarantees the dispersion of LDH in casting solutions.

Viscosity Measurement

The viscosity of the casting solution can affect the kinetics of phase inversion and can, thus, affect the resulting morphological structure and performance of the membrane. An appropriate viscosity in the casting solution is necessary for the formation of an asymmetric structure with a combination of spongelike pores and fingerlike pores. Therefore, the viscosities of the casting solutions with and without LDH were measured. Figure 2 shows the effect of different amounts of LDH on the polymer solution viscosity. It was obvious that the viscosity of the dope solution was affected enormously by the concentration of LDH. Within certain LDH doses, the addition of LDH increased the viscosity of the casting solution. This phenomenon may have been due to its enhanced interaction among PES molecules, PVP, DMAc, and LDH; this deteriorated the polymer chain flexibility or caused a decrease in the distributive freedom of the polymer in the dope solution.[32] As LDH with abundant exposed hydroxyl groups has a high surface area and surface energy, it could adsorb other compositions in the casting solution and increase the interaction between LDH and the polymers.[33] On the other hand, the positively charged LDH could

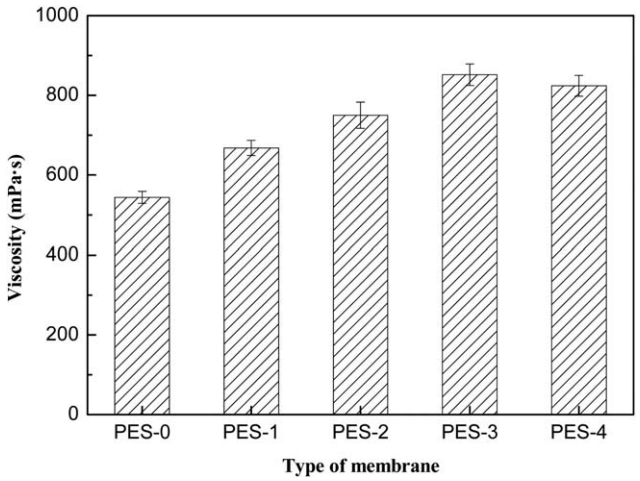

Figure 2. Effect of the Zn–Al LDH on the viscosity of the casting solutions.

also attract negatively charged polymer and enhance the interactions.

It has been reported that a higher viscosity can slow down the solvent–nonsolvent exchange rate and shift the path of phase inversion from instantaneous to a delayed liquid–liquid demising; this would suppress the formation of macrovoids.[34–36] However, the existence of hydrophilic additives, which have higher affinity to water than polymer, can enhance the penetration velocity of water into a nascent membrane and the solvent diffusion velocity from membrane to water and cause the formation of larger cavities.[34,37]

Because of the opposite effects on the phase-inversion process, the influence of Zn–Al LDH embedding in the final PES membrane structure requires further investigation.

Membrane Morphology

Figure 3 illustrates the cross-sectional images of the prepared PES membranes. Overall, Zn–Al LDH was dispersed relatively

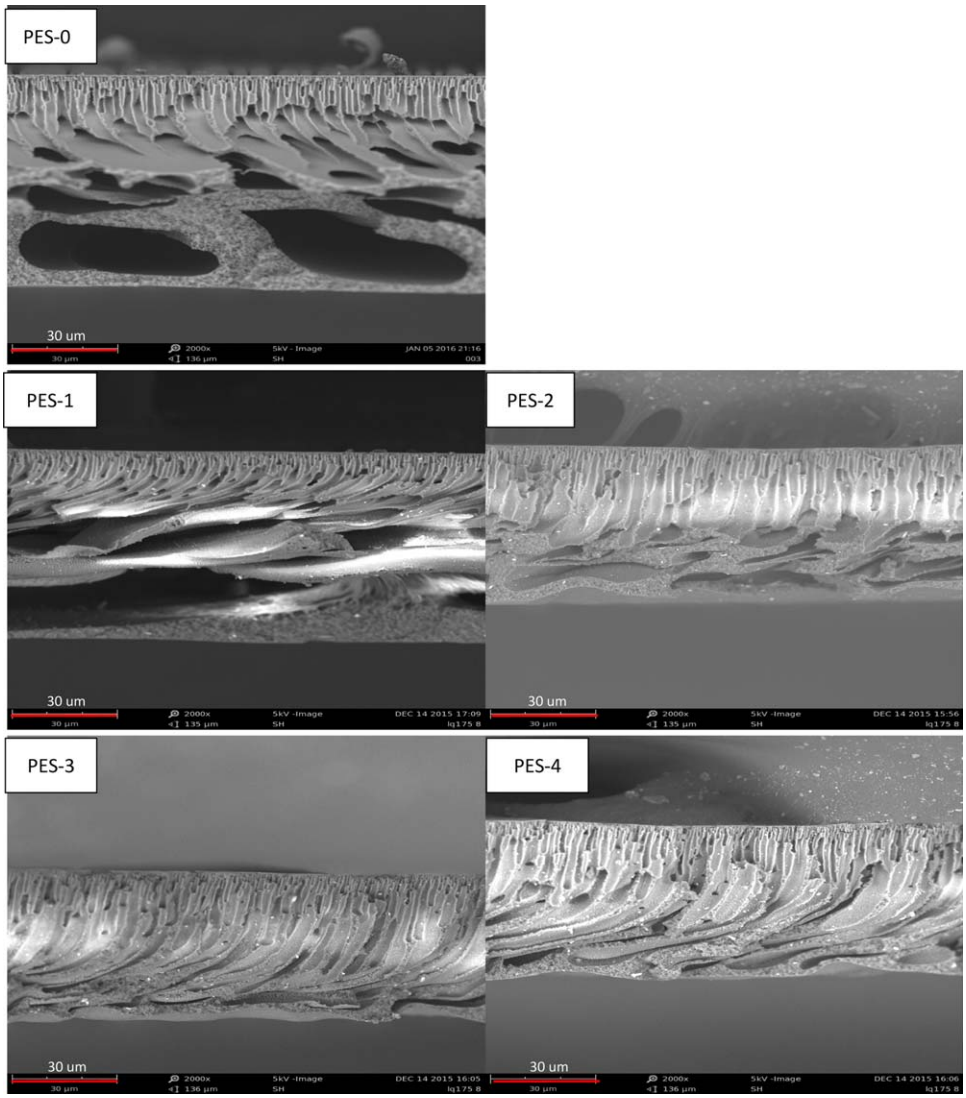

Figure 3. Cross-sectional morphologies of the PES membranes. [Color figure can be viewed in the online issue, which is available at wileyonlinelibrary.com.]

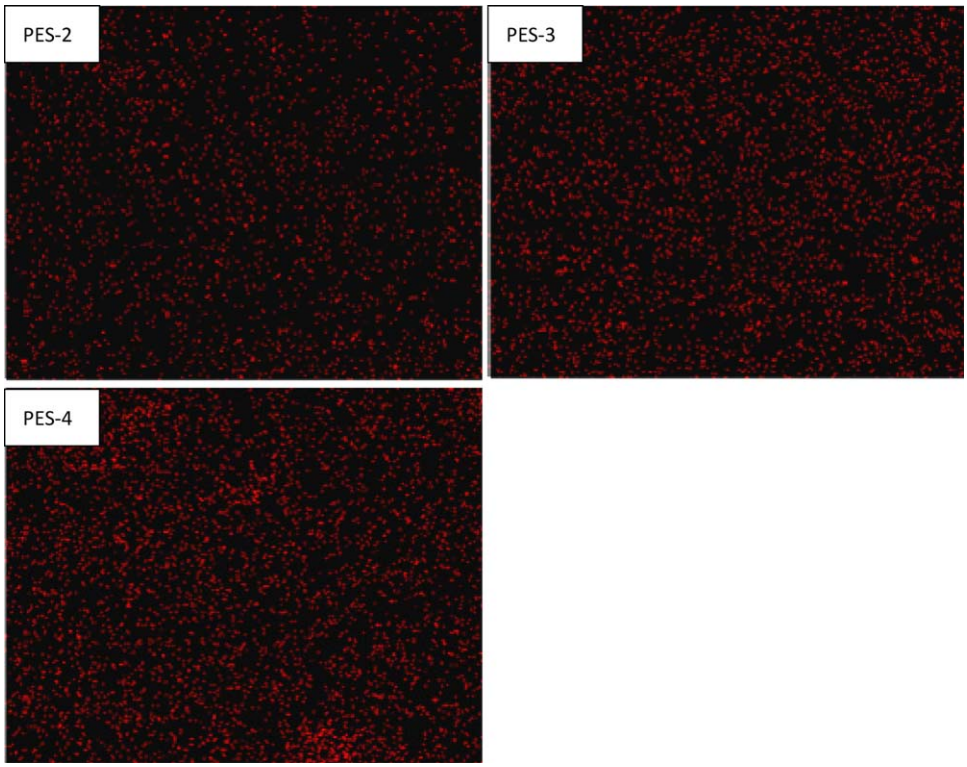

Figure 4. EDX mapping of Al on the PES membrane surfaces. [Color figure can be viewed in the online issue, which is available at wileyonlinelibrary.com.]

homogeneously in the PES membranes, and there were not obvious agglomerations of LDH. All of the PES membranes had a typical asymmetric structure and contained three layers, two skin layers at the top and bottom side of the membranes and one macrovoid layer in the middle, with fingerlike pores and macropores surrounded by spongelike pores. When the addition of LDH increased, the fingerlike pores extended further into the bottom side, the part with macropores became much thinner, and the size of the macropores became smaller and smaller before the content of LDH reached 2.0%. We also found that the integral thickness of the membrane decreased with the incorporation of LDH, and the macropores surrounded by spongelike pores were replaced with fingerlike pores. When the LDH content was increased further, the thickness of the PES membrane grew slightly, and the proportion of the fingerlike part did not increase further. We observed that the fingerlike voids penetrated through almost the whole film and led from the top side to the bottom side for PES-3 and PES-4. Moreover, the fingerlike pores in PES-4 were not as uniform as those in membranes with less LDH; this could have an effect on the rejection efficiency of foulants for membranes. The trend of macropore change in the membrane structure coincided with that of the casting solution viscosity change, with macropores disappearing gradually as the viscosity increased. Therefore, such an observation about the membrane structural change was ascribed to the increased solution viscosity, with a higher viscosity suppressing the formation of pores with larger sizes. However, in contrast to previous studies, the enhanced viscosity did not inhibit the growth of fingerlike pores and created more spongelike pores. On the contrary, the fingerlike pores extended deeper and penetrated through almost the whole film with increasing LDH. This may have been due to the high affinity to water of LDH.

Figure 4 shows the EDX mapping of Al on the surfaces of PES-2, PES-3, and PES-4. As shown, the amount of Al on the membrane surface increased with increasing LDH addition from 1.0 to 3.0%. For PES-2 and PES-3, the Al element was uniformly distributed, whereas for PES-4, there were obvious agglomerations; this indicated the uneven distribution of LDH in PES-4.

The membrane surface roughness is an important parameter in the characterization of the morphology of a membrane. Because a membrane with a higher roughness can accumulate contaminants on its surface more easily, membrane fouling increases with increasing roughness.[38]

The mean roughness and root mean square values of the data were calculated by NanoScope Analysis software in a 2.5 × 2.5 μm^2 scan size and are presented in Table II. According to the two- and three-dimensional graphs in Figure 5 and the surface roughness data in Table II, the incorporation of LDH produced a smoother surface compared to that of the pristine PES

Table II. Roughness Values of the PES-0 and PES-3 Membranes

	Roughness	
	Mean roughness (nm)	Root mean square (nm)
PES-0	11.20 ± 1.0	14.72 ± 2.1
PES-3	9.01 ± 1.2	12.48 ± 1.4

Scanning area = 2.5 × 2.5 μm^2.

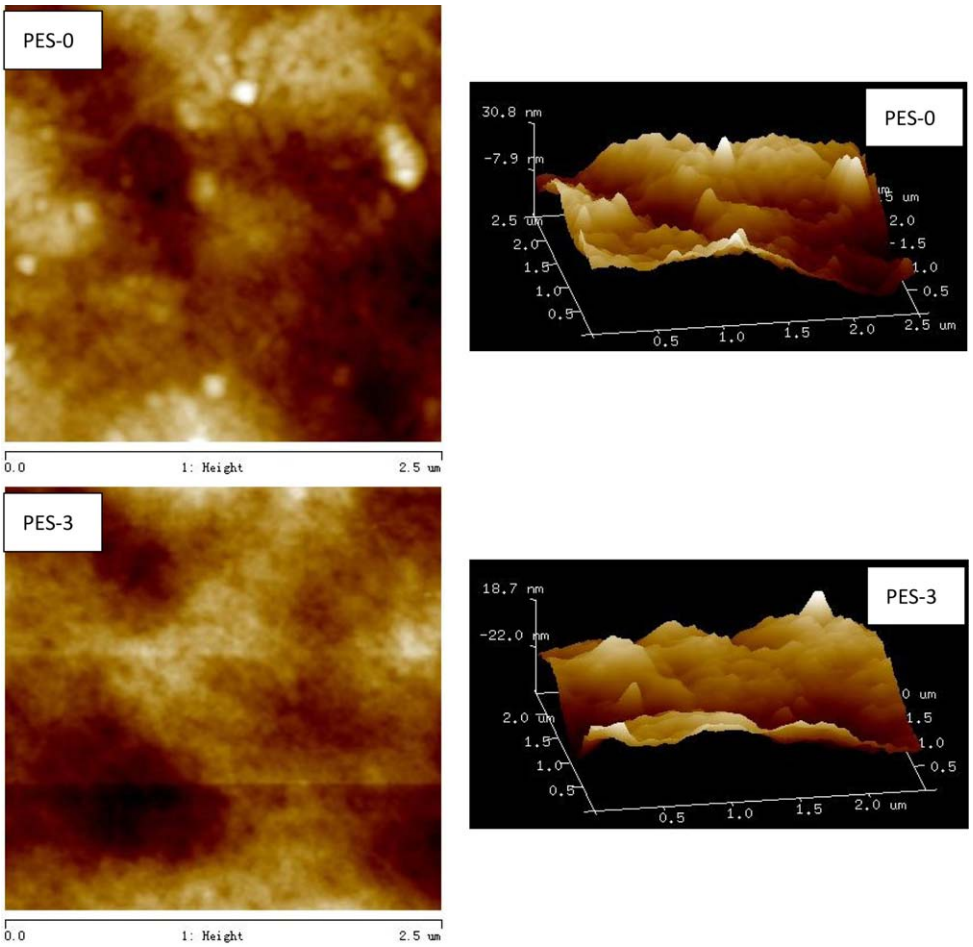

Figure 5. Two- and three-dimensional AFM micrographs of the PES-0 and PES-3 membranes. [Color figure can be viewed in the online issue, which is available at wileyonlinelibrary.com.]

membrane. In the scan range, the mean roughness values of the pristine and LDH-embedded membranes were 11.20 and 9.01 nm, respectively. Other researchers achieved similar results. Nanofillers such as carbon nantubes,[39] TiO_2,[30] and graphene oxide[40] endowed membranes with a lower surface roughness and, thus, better antifouling abilities.

CA and EWC

The hydrophilicity of a membrane is closely related to its water flux and antifouling ability.[41] To examine the hydrophilicity or hydrophobicity of the PES membranes, CA and EWC were measured. Small droplets of distilled water were deposited onto the surface of the dried PES membrane at five different points, and the reported CA values are the averages of five points taken to minimize experimental error.

Both the CA and EWC values are presented in Figure 6. Within a certain range, a greater LDH dose produced a smaller CA and higher EWC; this indicated a more hydrophilic surface. The variation trend was more obvious, especially when the concentration of LDH increased from 0 to 1.0%. The pure PES membrane possessed the highest water CA of 66.60°; this indicated its relatively high hydrophobicity and weak antifouling properties. With the addition of 0.5, 1.0, 2.0, and 3.0 wt % LDH, the CAs were reduced to 60.32, 53.09, 50.21, and 50.94° for the PES-1, PES-2, PES-3, and PES-4 membranes, respectively. As excess LDH loading could cause the agglomeration or irregular collocations of LDH nanoplates in the polymer matrix because of the existence of steric hindrance and electrostatic interactions between LDH and PES or LDH itself, the CA for PES-4 was slightly higher than that of PES-3.[42]

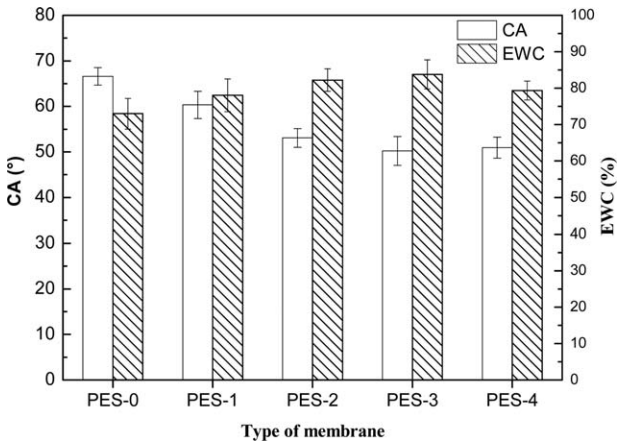

Figure 6. EWC and CA values of the PES membranes.

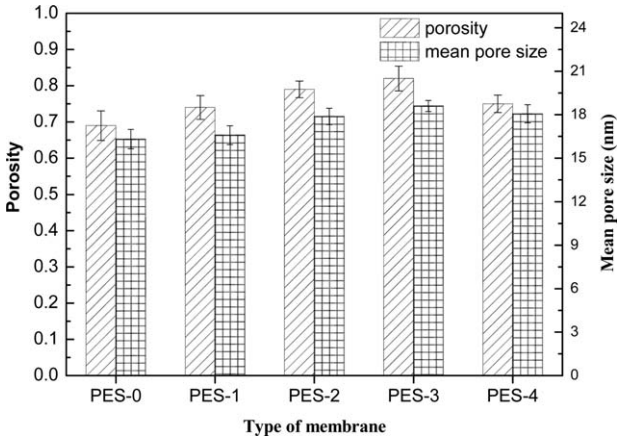

Figure 7. Porosity and mean pore size of the PES membranes.

The higher EWC values for membranes in the presence of LDH could have been caused by the hydrophilicity feature of LDH and the morphological structural changes in the membranes after the incorporation of the nanosheets. As shown in the SEM micrographs, the part with macropores and spongelike pores was transformed to a structure with fingerlike pores with many more wrinkles; this increased the water intake of the pores and enhanced the EWC. Furthermore, the structural variation of membranes was more evident when the LDH addition was below 2.0 wt %; this corresponded to a more obvious change in EWC. Actually, EWC represents the fraction of water molecules occupied in the pores of a membrane. So, the higher EWC values for the LDH-embedded membranes indicated its more porous properties.[41] Then, EWC decreased from 83.75 to79.37% with increasing LDH content from 2.0 to 3.0 wt %.

Porosity and Pore Size Measurement

The porosity is a vital indicator in the characterization of membranes. As it is difficult to obtain the actual pore size of a membrane, the parameter of mean pore size calculated on the basis of the porosity and pure water flux is usually used as an alternative. Figure 7 gives the membrane porosity and pore size data. We noticed that there was a gradual increase in the porosity and mean pore size with the addition of LDH to the polymer matrix at first and that a slight increase in the two parameters was observed when the LDH concentration reached 3.0%; this showed the same trend as CA and EWC. As is known, the porosity and average pore size increased with solvent interdiffusion velocity.[43] Compared with the unfilled PES membrane, the membranes with hydrophilic LDH had a much faster solvent and nonsolvent exchange rate during the phase-inversion process, and thus, they had higher membrane porosity and pore size values. Therefore, compared with the delayed effect of the casting solution viscosity increase, the acceleration effect of hydrophilic LDH on the phase inversion was more obvious.

Mechanical Strength Measurement

Because the mechanical strength of membranes is crucial for the practical application of water treatment, the tensile strength and elongation at break were measured. Table III lists the mechanical strength data of the membranes. The highest tensile strength and elongation at break were observed for PES-3.

It is well known that pores with larger sizes can yield mechanical weaknesses in membranes and, thus, are undesirable.[44] As shown in Figure 3, the presence of big voids in PES-0 may have affected the mechanical strength. On the other hand, LDH, with its abundant functional groups, could act as a crosslinking point in the composite membrane to link the polymer chain and increase the rigidity of the polymer chain; this means that more energy is required if the membrane is fractured.[45] The enhancement in the mechanical properties also indicated the relatively good miscibility of LDH in polymer matrix to some extent. If not, the weakening effect of the mechanical strength due to the existence of the void between the PES polymer and LDH would be much more evident and membranes with LDH would show a lower tensile strength and breaking elongation than the pristine PES membrane.[46]

Streaming Potential Evaluation

Electrical potential measurement was carried out to further investigate the membrane surface properties, and Figure 8 shows the results of the measurements for PES-0 and PES-3. The pure PES was negatively charged, as the polar groups on its surface could be ionized or PES molecules could adsorb surrounding anions selectively.[47] Hence, both of the two PES membranes exhibited negatively charged properties in the pH range 5–11. We also observed that the surface ζ potentials for the pure and blended PES membranes were pH dependent, with a higher pH value corresponding to a lower ζ potential in an overall sense. The difference between the two membranes was in the less negative surface of PES-3 compared to that of PES-0 because part of the incorporated positively charged Zn–Al LDH can be exposed to the outside. For example, the ζ potentials at pH 7 for PES-0 and PES-3 were -69.49 and -52.05 mV, respectively, and the values were -77.01 and -66.28 mV at pH 11. The relatively less negative membrane surface could have weakened the severe deposition of cationic foulants onto the membranes and, thus, weakened the membrane fouling to some extent.[48]

Protein Adsorption onto Membranes

Membrane fouling can be caused by various undesired interactions, such as electrostatic attraction, van der Waals interactions, and hydrogen bonding, between the membrane materials and typical colloids (e.g., proteins or oil droplets in water).[49,50] Here, we examined the antifouling properties of the PES membranes using static protein adsorption experiments with BSA

Table III. Tensile Strength and Breaking Elongation Values of the PES Membranes

Membrane type	Tensile strength (MPa)	Breaking elongation (%)
PES-0	4.16 ± 0.30	7.22± 0.38
PES-1	4.38 ± 0.27	8.68± 0.45
PES-2	4.53 ± 0.12	9.08± 0.22
PES-3	4.63 ± 0.23	9.20± 0.42
PES-4	4.40 ± 0.19	7.95± 0.37

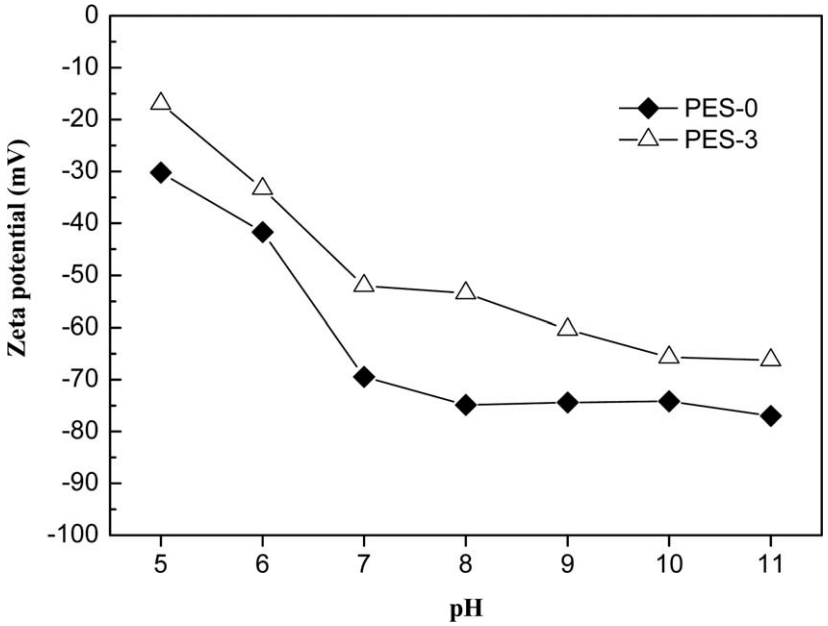

Figure 8. ζ potentials of the PES-0 and PES-3 membranes.

and LYS as model proteins. The adsorbed amounts of BSA and LYS for virgin and modified PES membranes are presented in Figure 9. As shown, PES-2 and PES-3 showed the lowest BSA and LYS adsorptions, respectively. Compared with the pristine PES membrane, the LDH-embedded membranes had hydration layers on their surfaces because of to the presence of hydrophilic LDH; consequently, protein adsorption onto them was inhibited because of the effect of steric exclusion.[51–53] As LDH and BSA were differently charged, the membranes with LDH could adsorb BSA onto them because of electrostatic attraction. So, the relatively higher LDH addition affected the antifouling ability of the membranes; this was observed in the adsorption results of PES-2 and PES-3, although PES-2 had a higher hydrophilicity (with a lower CA and higher EWC). In contrast, membranes with the best hydrophilicity showed the best foulant resistance ability for LYS. The equilibrium adsorption amount of LYS decreased from 30.27 to 11.34 μg/cm^2 as the LDH content increased from 0 to 3.0%; this was about 62.5% less than that of the virgin membrane. However, as a contaminant-like protein could adsorb onto the LDH nanoplates because of the pretty high surface area and surface energy of LDH, the adsorption enhancement effect could surpass the fouling resistance effect. These results suggest good protein resistance characteristics in the LDH-incorporated membranes when a proper amount of LDH was used.

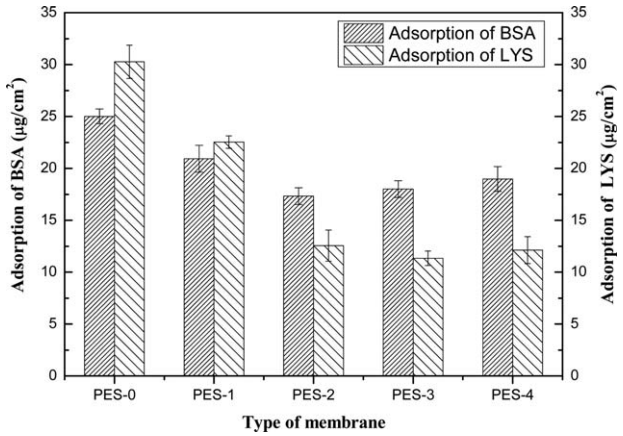

Figure 9. Static protein adsorption onto the PES membranes.

Filtration Experiments

Table IV reveals the pure water flux and rejection values of BSA and LYS for the prepared PES membranes with or without Zn–Al LDH. On the basis of Figure 5 and Table IV, the experimental data showed that the increasing trend of the pure water flux corresponded well with the CA and EWC change, and the hydrophilicity improved. The water flux increased from 80.21 to 119.10 L m^{-2} h^{-1} bar^{-1} with increasing LDH concentration from 0 to 2.0%; this was an approximately 48.5% enhancement. Further increases in the LDH content did not improve the water permeability more, just in accordance with the porosity and hydrophilicity reduction. As for the removal rate of BSA, all of the membranes showed excellent BSA removal with rejection rates above 99.0%. A slight reduction in the protein removal was also observed for BSA with increasing LDH from 2.0 to 3.0%; this was due to the reduction of electrostatic repulsion

Table IV. Pure Water Flux and Removal Rate Values of BSA and LYS

Membrane type	Pure water flux (L/m^2 h bar)	Removal of BSA (%)	Removal of LYS (%)
PES-0	80.21	99.59	79.23
PES-1	90.99	99.68	82.86
PES-2	111.59	99.82	88.69
PES-3	119.10	99.79	89.05
PES-4	113.75	99.63	89.34

and the stronger dominant electrostatic attraction. Because of the molecular mass and structure differences, although the removal rate for LYS was lower than that of BSA, the improvement degree of removal efficiency due to the existence of LDH was very obvious. Combined with the SEM images presented in Figure 3, the fingerlike pores in PES-4 were not as even as the others and, thus, could endow the membrane with better interception effects. Together with the relatively stronger electrostatic repulsion, PES-4 showed the highest LYS removal.

In summary, to obtain a desirable separation performance and water permeability, the addition of LDH nanoplates should be controlled at appropriate amounts.

CONCLUSIONS

Hydrophilic PES ultrafiltration membranes embedded with LDH were successfully prepared via a phase-inversion method. A series of characterizations of the LDH and prepared membranes were investigated; these characterizations included SEM, TEM, AFM, viscosity, water CA, EWC, porosity, average pore size, ζ potential, mechanical strength, antifouling ability, water permeation, and rejection property experiments. The experimental results reveal that the PES membranes were successfully modified with LDH and that the hybrid membranes exhibited significantly changed morphologies and evident hydrophilicity enhancements compared with the neat polymeric membrane. Membranes with LDH incorporation simultaneously achieved better water permeability, higher protein removal, and better antifouling abilities.

Although a series of characterizations of the PES membranes were done, future work still needs be done to explore further the membrane properties and the potential of these membranes for water treatment. For example, the removal efficiency and membrane-fouling characteristics of the hybrid membranes for use in natural water treatment are still unknown.

ACKNOWLEDGMENTS

Financial support from National Natural Science Foundation of China (Nos. 51378367 and 51578388) was greatly acknowledged. The study was also Supported by the Fundamental Research Funds for the Central Universities.

REFERENCES

1. Guo, W.; Ngo, H.-H.; Li, J. *Bioresour. Technol.* **2012**, *122*, 27.
2. Sonune, A.; Ghate, R. *Desalination* **2004**, *167*, 55.
3. Zhang, X.; Hu, Q.; Sommerfeld, M.; Puruhito, E.; Chen, Y. *Bioresour. Technol.* **2010**, *101*, 5297.
4. Zou, S.; Gu, Y.; Xiao, D.; Tang, C. Y. *J. Membr. Sci.* **2011**, *366*, 356.
5. Li, X.; Huang, J.; Zhang, Y.; Lv, Y.; Liu, Z.; Shu, Z. *Desalination and Water Treatment* **2016**, *57*, 10980.
6. Harisha, R.; Hosamani, K.; Keri, R.; Nataraj, S.; Aminabhavi, T. *Desalination* **2010**, *252*, 75.
7. Shi, Q.; Su, Y.; Zhu, S.; Li, C.; Zhao, Y.; Jiang, Z. *J. Membr. Sci.* **2007**, *303*, 204.
8. Wang, Y.-Q.; Wang, T.; Su, Y.-L.; Peng, F.-B.; Wu, H.; Jiang, Z.-Y. *Langmuir* **2005**, *21*, 11856.
9. Yang, Q.; Xu, Z.-K.; Dai, Z.-W.; Wang, J.-L.; Ulbricht, M. *Chem. Mater.* **2005**, *17*, 3050.
10. Taniguchi, M.; Belfort, G. *J. Membr. Sci.* **2004**, *231*, 147.
11. Schoeberl, P.; Brik, M.; Bertoni, M.; Braun, R.; Fuchs, W. *Sep. Purif. Technol.* **2005**, *44*, 61.
12. Fan, X.; Dong, Y.; Su, Y.; Zhao, X.; Li, Y.; Liu, J.; Jiang, Z. *J. Membr. Sci.* **2014**, *452*, 90.
13. Zhang, Y.; Su, Y.; Peng, J.; Zhao, X.; Liu, J.; Zhao, J.; Jiang, Z. *J. Membr. Sci.* **2013**, *429*, 235.
14. Kim, I.; Choi, J.; Tak, T. *J. Appl. Polym. Sci.* **1999**, *74*, 2046.
15. Pieracci, J.; Crivello, J. V.; Belfort, G. *J. Membr. Sci.* **2002**, *202*, 1.
16. Zhao, C.; Xue, J.; Ran, F.; Sun, S. *Prog. Mater. Sci.* **2013**, *58*, 76.
17. Bolong, N.; Ismail, A. F.; Salim, M. R.; Rana, D.; Matsuura, T. *J. Membr. Sci.* **2009**, *331*, 40.
18. Wang, Y.-Q.; Su, Y.-L.; Ma, X.-L.; Sun, Q.; Jiang, Z.-Y. *J. Membr. Sci.* **2006**, *283*, 440.
19. He, J.; Wei, M.; Li, B.; Kang, Y.; Evans, D. G.; Duan, X. Layered Double Hydroxides; Eds.; Springer: Berlin, **2006**; 119.
20. Azzouz, A.; Aruş, V.-A.; Platon, N.; Ghomari, K.; Nistor, I.-D.; Shiao, T. C.; Roy, R. *Adsorption* **2013**, *19*, 909.
21. Lakshmi Kantam, M.; Koteswara Rao, K. *Green Chem.* **2001**, *3*, 257.
22. Kozai, N.; Ohnuki, T.; Komarneni, S. *J. Mater. Res.* **2002**, *17*, 2993.
23. Cavani, F.; Trifirò, F.; Vaccari, A. *Catal. Today* **1991**, *11*, 173.
24. Hoek, E. M.; Ghosh, A. K.; Huang, X.; Liong, M.; Zink, J. I. *Desalination* **2011**, *283*, 89.
25. Balta, S.; Sotto, A.; Luis, P.; Benea, L.; Van der Bruggen, B.; Kim, J. *J. Membr. Sci.* **2012**, *389*, 155.
26. Shen, J.-N.; Ruan, H.-M.; Wu, L.-G.; Gao, C.-*J. Chem. Eng. J.* **2011**, *168*, 1272.
27. Liu, J.; Yu, L.; Zhang, Y. *Desalination* **2014**, *335*, 78.
28. Liu, F.; Yi, B.; Xing, D.; Yu, J.; Zhang, H. *J. Membr. Sci.* **2003**, *212*, 213.
29. Feng, C.; Wang, R.; Shi, B.; Li, G.; Wu, Y. *J. Membr. Sci.* **2006**, *277*, 55.
30. Hamid, N.; Ismail, A. F.; Matsuura, T.; Zularisam, A.; Lau, W. J.; Yuliwati, E.; Abdullah, M. S. *Desalination* **2011**, *273*, 85.
31. Liu, J.; Shen, X.; Zhao, Y.; Chen, L. *Ind. Eng. Chem. Res.* **2013**, *52*, 18392.
32. Mei, S.; Xiao, C.; Hu, X. *J. Appl. Polym. Sci.* **2011**, *120*, 557.
33. Wang, S.-L.; Wang, P.-C. *Colloids Surf. A* **2007**, *292*, 131.
34. Hong, J.; He, Y. *Desalination* **2012**, *302*, 71.
35. Smolders, C.; Reuvers, A.; Boom, R.; Wienk, I. *J. Membr. Sci.* **1992**, *73*, 259.
36. Soroko, I.; Livingston, A. *J. Membr. Sci.* **2009**, *343*, 189.
37. Vatanpour, V.; Madaeni, S. S.; Moradian, R.; Zinadini, S.; Astinchap, B. *J. Membr. Sci.* **2011**, *375*, 284.

38. Yu, L.-Y.; Xu, Z.-L.; Shen, H.-M.; Yang, H. *J. Membr. Sci.* **2009**, *337*, 257.
39. Ghaemi, N.; Madaeni, S. S.; Daraei, P.; Rajabi, H.; Shojaeimehr, T.; Rahimpour, F.; Shirvani, B. *J. Hazard. Mater.* **2015**, *298*, 111.
40. Xia, S.; Ni, M. *J. Membr. Sci.* **2015**, *473*, 54.
41. Arthanareeswaran, G.; Mohan, D.; Raajenthiren, M. *J. Membr. Sci.* **2010**, *350*, 130.
42. Qiu, S.; Wu, L.; Pan, X.; Zhang, L.; Chen, H.; Gao, C. *J. Membr. Sci.* **2009**, *342*, 165.
43. Bae, T.-H.; Tak, T.-M. *J. Membr. Sci.* **2005**, *249*, 1.
44. Van de Witte, P.; Dijkstra, P.; Van den Berg, J.; Feijen, J. *J. Membr. Sci.* **1996**, *117*, 1.
45. Li, J.-F.; Xu, Z.-L.; Yang, H.; Yu, L.-Y.; Liu, M. *Appl. Surf. Sci.* **2009**, *255*, 4725.
46. Amirilargani, M.; Sadrzadeh, M.; Mohammadi, T. *J. Polym. Res.* **2010**, *17*, 363.
47. Pujar, N. S.; Zydney, A. L. *J. Colloid Interface Sci.* **1997**, *192*, 338.
48. Dong, H.; Wu, L.; Zhang, L.; Chen, H.; Gao, C. *J. Membr. Sci.* **2015**, *494*, 92.
49. Zhao, Y.-H.; Zhu, B.-K.; Kong, L.; Xu, Y.-Y. *Langmuir* **2007**, *23*, 5779.
50. Liu, S. X.; Kim, J.-T. *J. Adhes. Sci. Technol.* **2011**, *25*, 193.
51. Zhao, X.; Ma, J.; Wang, Z.; Wen, G.; Jiang, J.; Shi, F.; Sheng, L. *Desalination* **2012**, *303*, 29.
52. Upadhyayula, V. K.; Gadhamshetty, V. *Biotechnol. Adv.* **2010**, *28*, 802.
53. Wang, Y.-Q.; Wang, T.; Su, Y.-L.; Peng, F.-B.; Wu, H.; Jiang, Z.-Y. *J. Membr. Sci.* **2006**, *270*, 108.